

Three-Dimensional Chiral Microporous Germanium Antimony Sulfide with Ion-Exchange Properties**

Mei-Ling Feng, De-Nian Kong, Zai-Lai Xie, and Xiao-Ying Huang*

Microporous materials have widespread applications in catalysis, molecular recognition, separations, and ion exchange.^[1] Extensive interest has focused on open-framework metal chalcogenides owing to the porosity, fascinating architectures and topologies, and their potential applications in areas such as fast-ion conductivity, photocatalysis, electro-optics, chemical sensors, thermoelectrics, and molecular electronics.^[2] Among porous metal chalcogenides, typical examples are those based on the supertetrahedral clusters (T_n , P_n , C_n) with tunable components and sizes of the secondary building units (SBU).^[2a–f] Heterometallic chalcogenides involving transition metals and main-group metals have also been described.^[3] Although Group 13 and Group 15 metal chalcogenides have been reported,^[4] open-framework chalcogenides constructed with SBU integrating both tetrahedra and other polyhedra of main-group metals, in particular those possessing asymmetric coordination geometry, are less explored.^[5,6] The compound $[(CH_3CH_2CH_2)_2NH_2]_5In_5Sb_6S_{19} \cdot 1.45H_2O$ contains Group 13 metal tetrahedra and Group 15 metal trigonal pyramids.^[6] However, open-framework chalcogenides incorporating Group 15 metal asymmetric coordination polyhedra and Group 14 metal tetrahedra have not been to date documented.

Chiral open frameworks in solid materials are especially desirable for enantioselective separation and catalysis.^[7] Most chiral open frameworks discovered to date are oxide-based materials;^[7c,d] however, chalcogenide-based materials-associated porous chiral structures with semiconducting and optoelectronic properties are quite limited.^[8] Studies indicate that the asymmetric coordination geometry adopted by the ions (such as Se^{4+} , Te^{4+} , Sb^{3+}) with stereochemically active electron lone pairs can induce noncentrosymmetric struc-

tures, which may result in interesting physical properties, such as second-harmonic generation.^[9] Our approach was to integrate main-group metal tetrahedra with Group 15 metal asymmetric coordination polyhedra, such as $[Sb^{III}Q_n]^{x-}$ ($Q = S, Se$; $n = 3, 4$; $x = 3, 5$), in the presence of organic amines as structure-directing agents. Such an approach would lead to the formation of various heterometallic SBU giving rise to novel open-framework chalcogenides with diverse topologies. Furthermore, the stereochemically active lone pairs of antimony(III) are likely to induce structures with noncentrosymmetric or even chiral features. Herein we present the first chiral microporous germanium antimony sulfide, $[(Me)_2NH_2]_2[Sb_2GeS_6]$ (**1**). Investigation of the ion-exchange properties indicates that **1** has high ion-exchange capacity and high selectivity for Cs^+ ions, and is thus a material with the potential for remediation of radioactive Cs^+ ions from nuclear-waste solutions.^[6,10]

Yellow prismatic crystals of **1** were obtained by solvothermal reaction of GeO_2 , sulfur, and antimony in N,N' -dimethylformamide (DMF) at 160 °C for 7 days. In this reaction, the solvent DMF was hydrolyzed to produce dimethylammonium ions in situ. The in-situ synthesis of dimethylammonium ion is of significance for the preparation of **1**, as the same reaction in dimethylamine or dimethylammonium chloride in water instead of DMF yielded powders that could not be accurately characterized. Single-crystal X-ray analysis reveals that **1** crystallizes in the chiral space group $P4_212$ with a three-dimensional network containing 3D chiral channels (Figure 1a). The asymmetric unit of **1** contains half of a Ge^{4+} ion located at the special position with two-fold symmetry (on $4c$ site), one unique Sb^{3+} ion, three S^{2-} ions, and one dimethylammonium cation. The Ge^{4+} ion is tetrahedrally coordinated to two S(2) and two S(3) atoms. The Sb^{3+} ion adopts a ψ - $[SbS_4]$ trigonal bipyramidal coordination geometry with two short (2.4468(12) and 2.4652(12) Å) and two long (2.6931(13) and 2.8368(13) Å) Sb–S distances, in which two long Sb–S bonds are nearly *trans* to each other; the fifth coordination site is occupied by the lone pairs of the antimony(III). Each S^{2-} anion acts as a bidentate metal linker: S(1) bridges two Sb atoms, S(2) and S(3) connect with one Ge and one Sb atom, respectively. The ψ - $[SbS_4]$ trigonal bipyramids are interconnected by sharing a corner S(1) atom to form a left-handed helical chain running along the 4_1 axis parallel to the c axis (Figure 1b,c). These Sb–S–Sb left-handed helices are further weaved using $[GeS_4]$ tetrahedra, and another type of left-handed helical chains are formed. These helices run along the 2_1 axis parallel to the c axis, and are formed by alternating arrays of $[GeS_4]$ tetrahedra and ψ - $[SbS_4]$ trigonal bipyramids by corner-sharing (Figure 1d,e). These chiral channels in Figure 1d, with a rough square cross-

[*] Dr. M.-L. Feng, D.-N. Kong, Z.-L. Xie, Prof. Dr. X.-Y. Huang
State Key Laboratory of Structural Chemistry
Fujian Institute of Research on the Structure of Matter
Chinese Academy of Sciences
Fuzhou, Fujian 350002 (P. R. China)
Fax: (+86) 591-8379-3727
E-mail: xyhuang@fjirsm.ac.cn
Homepage: <http://xyhuang.fjirsm.ac.cn/>

[**] This work was supported by grants from the 973 Program (No. 2006CB932904), the NNSF of China (Nos. 20771102, 20873149, 20803081), the NSF of Fujian Province (No. 2008J0174), YIF of Fujian Province (No. 2007F3114), the State Key Laboratory of Structural Chemistry (No. 20080042), the Scientific Research Foundation of the State Human Resource Ministry, and the Fujian Institute of Research on the Structure of Matter, Chinese Academy of Sciences (CAS).

Supporting information for this article is available on the WWW under <http://dx.doi.org/10.1002/anie.200803406>.

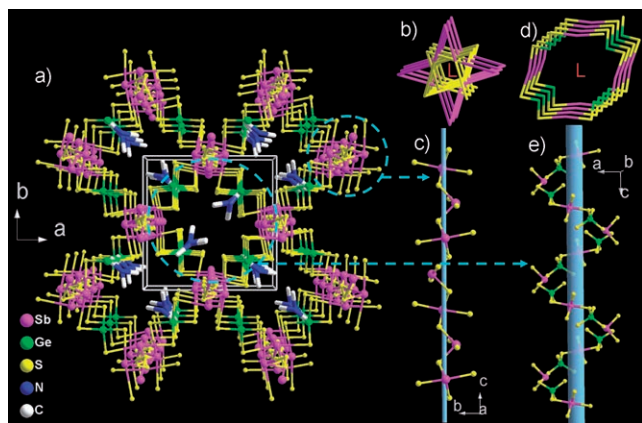


Figure 1. a) View of the structure of **1** along the *c* axis. b) The cross-section, and c) the profile of a left-handed helical chain running along the 4_1 axis parallel to the *c* axis formed by corner-sharing ψ - $\{\text{SbS}_4\}$ trigonal bipyramids. d) The cross-section, and e) the profile of a left-handed helical chain running along the 2_1 axis parallel to the *c* axis formed by the alternating array of $\{\text{GeS}_4\}$ tetrahedra and ψ - $\{\text{SbS}_4\}$ trigonal bipyramids by a corner-sharing sulfur atom.

section of $6.37 \times 5.46 \text{ \AA}^2$, are evidently parallel to the *c* axis. One full turn of the Sb–S–Sb and Ge–S–Sb left-handed helices contains four $\{\text{SbS}_4\}$ and eight polyhedra (four $\{\text{GeS}_4\}$ and four $\{\text{SbS}_4\}$ units), respectively. Both helices have a pitch of 13.81 Å. Each Sb–S–Sb left-handed helix (symmetry 4_1) connects to four Ge–S–Sb left-handed helices (symmetry 2_1) by sharing one fourth of the ψ - $\{\text{SbS}_4\}$ polyhedra to generate a 3D anionic network of $[\text{Sb}_2\text{GeS}_6]^{2-}$.

Compound **1** contains intersected channels parallel to the *a* or *b* axis (Figure 2a), and two types of helical chains of opposite chirality are found running along these axes. Three $\{\text{SbS}_4\}$ groups form one $\{\text{Sb}_3\text{S}_{10}\}$ unit by corner-sharing and these units are linked by $\{\text{GeS}_4\}$ tetrahedra in a bidentate fashion to form a left-handed helix of an alternating array of $\{\text{GeS}_4\}$ and $\{\text{Sb}_3\text{S}_{10}\}$ (Figure 2b). $\{\text{GeS}_4\}$ tetrahedra linking the middle $\{\text{SbS}_4\}$ groups of $\{\text{Sb}_3\text{S}_{10}\}$ units by corner-sharing, on

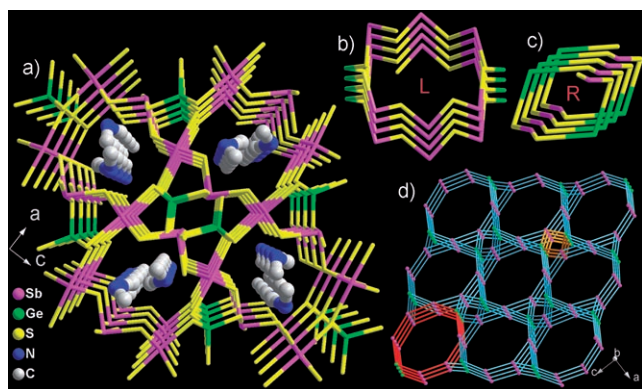


Figure 2. a) View of the structure of **1** along the *b* axis. The dimethylammonium cations are located in the chiral channels. b) The left-, and c) right-handed helical chains are parallel to the *b* axis. d) Schematic view of the $(3^2 \cdot 10^4)$ net in the structure of **1** along the *b* axis, the $\{\text{GeS}_4\}$ and $\{\text{SbS}_4\}$ (green/magenta) function as 4-connected nodes. The highlighted parts are left- (red) and right-handed (orange) helices parallel to the *b* axis.

the other hand, lead to a right-handed helix of an alternating $\{\text{GeS}_4\}$ and ψ - $\{\text{SbS}_4\}$ arrays (Figure 2c). One full turn of the left- and right-handed helices include eight (two $\{\text{GeS}_4\}$ and six $\{\text{SbS}_4\}$) and four polyhedra (two $\{\text{GeS}_4\}$ and two $\{\text{SbS}_4\}$), respectively. Both helices have a pitch of 10.99 Å. A nearly hexagonal channel with a cross-section of $7.68 \times 5.65 \text{ \AA}^2$ is located in the left-handed helical chain. The dimethylammonium cations are found in the channels and form N–H···S hydrogen bonds with the sulfur atoms of the anionic frameworks. The solvent-accessible volume excluding the dimethylammonium cations in **1** is 45.2%.^[11] From the topological point of view, the 3D network of **1** is a $3^2 \cdot 10^4$ topology built upon a 4-connected net (Figure 2d), in which both $\{\text{GeS}_4\}$ and $\{\text{SbS}_4\}$ act as the 4-connected nodes. The long topological (O’Keeffe) vertex symbol of this $3^2 \cdot 10^4$ net is $3 \cdot 3 \cdot 10_2 \cdot 10_2 \cdot 10_3 \cdot 10_3$.^[12]

Although some thioantimonates and selenidoantimonates based on the asymmetrically coordinated $[\text{Sb}^{\text{III}}\text{Q}_n]^{x-}$ ($\text{Q} = \text{S}, \text{Se}; n = 3, 4; x = 3, 5$) units crystallized in chiral space groups,^[13] high-dimensional chiral porous chalcogenides were rarely isolated. Compound **1** is the first member of the three-dimensional metal chalcogenides with helical channels based on the combination of $\{\text{GeS}_4\}$ tetrahedra and ψ - $\{\text{SbS}_4\}$ asymmetric coordination geometries.

The three-dimensional chiral open channels in **1** are well-suited to ion exchange, and our experiments proved that the organic cations in **1** can be partially exchanged by alkali-metal cations, such as Cs^+ , Rb^+ , K^+ , and Na^+ ions in aqueous solutions. The elemental analysis and the exchange yields of the ion-exchange products are given in the Supporting Information. Within a single ion-exchange step under ambient conditions with CsCl in water, Cs^+ ions could replace up to about 93% of the organic cations in **1**. This result was confirmed by powder X-ray diffraction and elemental analysis. Single-crystal X-ray data and elemental analysis (Table S3) of **1** and its ion-exchanged product (**1Cs**) show that the solvent molecules (water) also enter the channels of the germanium antimony sulfide framework in addition to the Cs^+ ions. Similarly, about 85, 75, and 34% of the organic cations were exchanged by Rb^+ , K^+ , and Na^+ ions, respectively. Interestingly, the competitive ion-exchange experiments indicated that **1** had a strong preference for Cs^+ ions. Using equimolar amounts of alkali-metal cations Na^+ , K^+ , Rb^+ , and Cs^+ in a competitive ion-exchange reaction, only Rb^+ and Cs^+ ions were exchanged, and the exchange yield of Cs^+ ions was 5.8 times greater than that of Rb^+ . Using a molar 10:10:10:1 ratio of Na^+ , K^+ , Rb^+ , and Cs^+ in a competitive ion-exchange reaction, the K^+ , Rb^+ , and Cs^+ ions were exchanged with the respective yield ratio of 1:4.6:6.3 in the final ion-exchanged product. Thus, despite the initial 10-fold excess of Rb^+ over Cs^+ ion, the amount of Cs^+ was obviously more than that of Rb^+ in the ion-exchange product. Another competitive exchange experiment with a 20:1 molar ratio of $\text{Na}^+:\text{Cs}^+$ gave the product with only Cs^+ exchange. The selectivity of **1** for Cs^+ ions is higher than those of the reported metal chalcogenides.^[6,14] The excellent ion-exchange properties of **1** can be attributed to its open framework with three-dimensional chiral channels, which enable the guest cations to diffuse in and out of the material. The ion-exchange

capacity of **1** falls along with the decreasing radii of Cs^+ , Rb^+ , K^+ , and Na^+ ions, that is, the softer Lewis acidic cations are preferred over harder ones. This could be related with the soft basic nature of the framework in **1** and the size difference between the Me_2NH_2 cations and the replacing alkali cations.^[6] We also carried out Sr^{2+} ion-exchange experiment of **1**. Only trace amounts of Sr^{2+} was exchanged, probably owing to the bivalence of the alkaline earth metal. Scanning electronic microscope (SEM) examinations indicate that crystals of the pristine compound **1** possess relatively clean surfaces. After the ion-exchange step with Cs^+ , surface roughness appears; the crystals, however, retain their original shape (Figure 3).

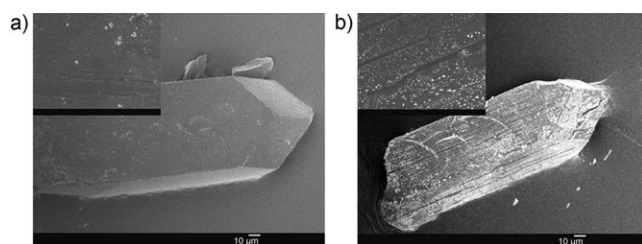


Figure 3. SEM images of a) the pristine compound and b) the Cs^+ ion-exchanged product. Insets are the magnified images of the surfaces of the crystals.

As shown in Figure 4, the optical absorption edge of **1** is 2.62 eV, which is suggestive of **1** being a semiconductor. The optical absorption edges for Cs^+ -, Rb^+ -, K^+ -, and Na^+ -exchanged products are 2.16, 1.90, 1.70, and 2.05 eV, respectively, consistent with their change in color. These band gaps lie in the energy range suitable for visible-light photocatalytic applications.^[15] The band gaps of the ion-exchanged products have a significant red shift compared to that of **1**. In particular, the band gap of the K^+ -exchanged product shows a red shift as large as 0.92 eV, which is rarely observed for ion-exchanged chalcogenides.^[3d,6,14] The red shift of the band gaps is probably due to the stronger bonding interactions of the smaller alkali metal ions with the sulfur atoms of the

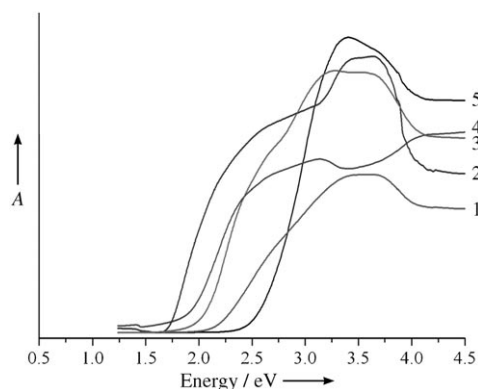


Figure 4. Optical absorption spectra of $[\text{Me}_2\text{NH}_2]_2[\text{Sb}_2\text{GeS}_6]$ (**5**) and the Cs^+ (**1**), Rb^+ (**4**), K^+ (**2**), Na^+ (**3**)-exchanged products for the single ion-exchange experiments.

framework in comparison to those between the larger alkali-metal or $[\text{Me}_2\text{NH}_2]^+$ ions and the sulfur atoms.^[16] A smaller red shift of the band gap of Na^+ -exchanged product compared to those of K^+ , Rb^+ -exchanged products might be due to its low exchange yield.

The ion-exchange properties of **1** were further confirmed by thermogravimetric analysis (TGA; Supporting Information Figure S13). The thermal stabilities of **1** and the ion-exchanged products were examined by TGA in a N_2 atmosphere from 30 to 500 °C. TGA curve of **1** displays one main weight-loss step, which corresponds to the loss of two dimethylammonium ions and one H_2S molecule. The observed weight loss of 20.8% is very close to the theoretical value of 20.7%. TGA curves of the Cs^+ -, Rb^+ -, and K^+ -exchanged products show respective weight losses of only 7.6%, 10.3% and 12.0% in the temperature range 30–500 °C, and are mostly due to the losses of the absorbed water, the unexchanged dimethylammonium ions and a small quantity of H_2S molecules.

In conclusion, the first 3D chiral microporous germanium antimony sulfide templated by in-situ-generated organic amines has been solvothermally synthesized. The combination of $\{\text{GeS}_4\}$ tetrahedral, and $\psi\text{-}\{\text{SbS}_4\}$ asymmetric coordination geometries in a single structure with 3D chiral channels is unprecedented, and may lead to heterometallic chalcogenide building blocks. Furthermore, **1** is an ion-exchange material for alkali metal cations, and is a new material for remediation of radioactive Cs^+ from nuclear wastes. It is anticipated that the synthetic approach described here can be used to develop new chiral semiconductor functional materials.

Experimental Section

1: A mixture of GeO_2 (1.0 mmol, 0.106 g), Sb (1.0 mmol, 0.123 g), and S (8.5 mmol, 0.274 g) in DMF (4 mL) was stirred under ambient conditions. The resulting mixture was sealed in a 20 mL stainless-steel reactor with a teflon liner, heated at 160 °C for 7 days, and then cooled to room temperature. Yellow prismatic crystals of **1** (along with an undefined amorphous yellow powder) were obtained by filtration. The crystals were selected by hand, washed with ethanol, and air-dried (yield: 0.052 g, 17.3% based on Sb). Elemental analysis calcd (%) for $\text{C}_4\text{H}_{16}\text{GeN}_2\text{S}_6\text{Sb}_2$ **1**: C 8.00, H 2.68, N 4.66, S 32.03; found: C 7.66, H 2.38, N 4.54, S 31.74.

A typical ion-exchange experiment was performed as follows: An excess of solid ACl ($\text{A} = \text{Na}, \text{K}, \text{Rb}, \text{Cs}$; 2 mmol) was dissolved in deionized water (20 mL), and $[\text{Me}_2\text{NH}_2]_2[\text{Sb}_2\text{GeS}_6]$ (**1**; ca. 0.02 mmol) was added to the salt solutions. The mixture was stirred at room temperature for 24 h. The exchanged products were then isolated in air by filtration and washed with deionized water, ethanol, and acetone.

Crystal data for **1**: $\text{C}_4\text{H}_{16}\text{GeN}_2\text{S}_6\text{Sb}_2$, $M_r = 600.64$, tetragonal, $P4_212$, $a = 10.988(3)$, $c = 13.808(6)$ Å, $V = 1667.0(9)$ Å³, $Z = 4$, $\rho_{\text{calc}} = 2.393$ g cm⁻³, $F(000) = 1136$, $\mu = 5.735$ mm⁻¹, $6^\circ \leq 2\theta \leq 55^\circ$, $T = 293(2)$ K, 12810 reflections measured, 1911 unique ($R_{\text{int}} = 0.021$), 1877 observed [$I > 2\sigma(I)$] with $R1(wR2) = 0.023(0.055)$, $R1(wR2) = 0.023(0.055)$ (all data). GOF = 1.08. Abs. struc.: 0.02(2). Crystal dimensions: 0.20 × 0.20 × 0.15 mm.

Crystal data for **1Cs**: $\text{C}_{0.38}\text{H}_{7.50}\text{Cs}_{1.81}\text{GeN}_{0.19}\text{O}_3\text{S}_6\text{Sb}_2$, $M_r = 812.04$, tetragonal, $P4_212$, $a = 10.7670(6)$, $c = 13.8760(14)$ Å, $V = 1608.6(2)$ Å³, $Z = 4$, $\rho_{\text{calc}} = 3.353$ g cm⁻³, $F(000) = 1459$, $\mu = 9.996$ mm⁻¹, $4^\circ \leq 2\theta \leq 55^\circ$, $T = 293(2)$ K, 5587 reflections measured,

1819 unique ($R_{\text{int}} = 0.046$), 1611 observed [$I > 2\sigma(I)$] with $R1(wR2) = 0.040(0.079)$, $R1(wR2) = 0.047(0.083)$ (all data). GOF = 1.11. Abs. struc.: 0.08(4). Crystal dimensions: $0.26 \times 0.06 \times 0.05$ mm.

The intensity data were collected on a Rigaku Mercury CCD diffractometer for **1** and a Rigaku SCXmini CCD diffractometer for **1Cs** with graphite-monochromated $\text{MoK}\alpha$ radiation ($\lambda = 0.71073$ Å) at room temperature. The structures were solved by direct methods and refined by full-matrix least-squares on F^2 using the SHELX97 program package.

CCDC-667663 (**1**) and CCDC-694036 (**1Cs**) contain the supplementary crystallographic data for this paper. These data can be obtained free of charge from The Cambridge Crystallographic Data Centre via www.ccdc.cam.ac.uk/data_request/cif.

Received: July 14, 2008

Published online: October 8, 2008

Keywords: antimony · germanium · ion exchange · microporous materials · sulfur

- [1] a) A. K. Cheetham, G. Férey, T. Loiseau, *Angew. Chem.* **1999**, *111*, 3466–3492; *Angew. Chem. Int. Ed.* **1999**, *38*, 3268–3292; b) M. E. Davis, *Nature* **2002**, *417*, 813–821; c) M. W. Anderson, T. Ohsuna, Y. Sakamoto, Z. Liu, A. Carlsson, O. Terasaki, *Chem. Commun.* **2004**, 907–916; d) C. S. Cundy, P. A. Cox, *Chem. Rev.* **2003**, *103*, 663–701; e) D. Maspoch, D. Ruiz-Molina, J. Veciana, *Chem. Soc. Rev.* **2007**, *36*, 770–919.
- [2] a) H. Li, A. Laine, M. O’Keeffe, O. M. Yaghi, *Science* **1999**, *283*, 1145–1147; b) H. Li, J. Kim, T. L. Groy, M. O’Keeffe, O. M. Yaghi, *J. Am. Chem. Soc.* **2001**, *123*, 4867–4868; c) N. Zheng, X. Bu, B. Wang, P. Feng, *Science* **2002**, *298*, 2366–2369; d) N. Zheng, X. Bu, P. Feng, *Nature* **2003**, *426*, 428–432; e) X. Bu, N. Zheng, P. Feng, *Chem. Eur. J.* **2004**, *10*, 3356–3362; f) P. Feng, X. Bu, N. Zheng, *Acc. Chem. Res.* **2005**, *38*, 293–303; g) S. Bag, P. N. Trikalitis, P. J. Chupas, G. S. Armatas, M. G. Kanatzidis, *Science* **2007**, *317*, 490–493; h) M. G. Kanatzidis, *Adv. Mater.* **2007**, *19*, 1165–1181; i) N. Hüsing, *Angew. Chem.* **2008**, *120*, 2018–2020; *Angew. Chem. Int. Ed.* **2008**, *47*, 1992–1994.
- [3] a) W. P. Su, X. Y. Huang, J. Li, H. X. Fu, *J. Am. Chem. Soc.* **2002**, *124*, 12944–12945; b) A. V. Powell, S. Boissière, A. M. Chippindale, *J. Chem. Soc. Dalton Trans.* **2000**, 4192–4195; c) S. Dehnen, M. K. Brandmayer, *J. Am. Chem. Soc.* **2003**, *125*, 6618–6619; d) N. Ding, D.-Y. Chung, M. G. Kanatzidis, *Chem. Commun.* **2004**, 1170–1171; e) V. Spetzler, C. Näther, W. Bensch, *Inorg. Chem.* **2005**, *44*, 5805–5812; f) S. Dehnen, M. Melullis, *Coord. Chem. Rev.* **2007**, *251*, 1259–1280.
- [4] a) W. S. Sheldrick, M. Wachhold, *Angew. Chem.* **1997**, *109*, 214–234; *Angew. Chem. Int. Ed. Engl.* **1997**, *36*, 206–224; b) W. S. Sheldrick, M. Wachhold, *Coord. Chem. Rev.* **1998**, *176*, 211–322; c) W. S. Sheldrick, *J. Chem. Soc. Dalton Trans.* **2000**, 3041–3052; d) J. Wachter, *Angew. Chem.* **1998**, *110*, 782–800; *Angew. Chem. Int. Ed.* **1998**, *37*, 750–768; e) P. Vaqueiro, M. L. Romero, *J. Phys. Chem. Solids* **2007**, *68*, 1239–1243.
- [5] A. Assoud, N. Soheilnia, H. Kleinke, *J. Solid State Chem.* **2004**, *177*, 2249–2454.
- [6] N. Ding, M. G. Kanatzidis, *Chem. Mater.* **2007**, *19*, 3867–3869.
- [7] a) P. R. Kavasmaneck, W. A. Banner, *J. Am. Chem. Soc.* **1977**, *99*, 44–50; b) C. E. Song, S.-g. Lee, *Chem. Rev.* **2002**, *102*, 3495–3524; c) O. R. Evans, D. R. Manke, W. Lin, *Chem. Mater.* **2002**, *14*, 3866–3874; d) C. Wu, A. Hu, L. Zhang, W. Lin, *J. Am. Chem. Soc.* **2005**, *127*, 8940–8941.
- [8] a) H. Ahari, A. Lough, S. Petrov, G. A. Ozin, R. L. Bedard, *J. Mater. Chem.* **1999**, *9*, 1263–1274; b) C. Wang, X. Bu, N. Zheng, P. Feng, *Chem. Commun.* **2002**, 1344–1345; c) J.-H. Liao, G. M. Marking, K. F. Hsu, Y. Matsushita, M. D. Ewbank, R. Borwick, P. Cunningham, M. J. Rosker, M. G. Kanatzidis, *J. Am. Chem. Soc.* **2003**, *125*, 9484–9493; d) Q. Zhang, X. Bu, J. Zhang, T. Wu, P. Feng, *J. Am. Chem. Soc.* **2007**, *129*, 8412–8413; e) I. Chung, C. D. Malliakas, J. I. Jang, C. G. Canlas, D. P. Weliky, M. G. Kanatzidis, *J. Am. Chem. Soc.* **2007**, *129*, 14996–15006; f) J. Zhou, G.-Q. Bian, J. Dai, Y. Zhang, A.-B. Tang, Q.-Y. Zhu, *Inorg. Chem.* **2007**, *46*, 1541–1543; g) M.-L. Fu, G.-C. Guo, X. Liu, J.-P. Zou, G. Xu, J.-S. Huang, *Cryst. Growth Des.* **2007**, *7*, 2387–2389; h) Y. Wu, W. Bensch, *Inorg. Chem.* **2007**, *46*, 6170–6177; i) M. J. Manos, J. I. Jang, J. B. Ketterson, M. G. Kanatzidis, *Chem. Commun.* **2008**, 972–974; j) Q. Zhang, Z. Lin, X. Bu, T. Wu, P. Feng, *Chem. Mater.* **2008**, *20*, 3239–3241.
- [9] a) K. M. Ok, E. O. Chi, P. S. Halasyamani, *Chem. Soc. Rev.* **2006**, *35*, 710–717; b) E. O. Chi, K. M. Ok, Y. Porter, P. S. Halasyamani, *Chem. Mater.* **2006**, *18*, 2070–2074; c) F. Kong, S.-P. Huang, Z.-M. Sun, J.-G. Mao, W.-D. Cheng, *J. Am. Chem. Soc.* **2006**, *128*, 7750–7751.
- [10] a) E. A. Behrens, D. M. Poojary, A. Clearfield, *Chem. Mater.* **1996**, *8*, 1236–1244; b) A. I. Bortun, L. N. Bortun, D. M. Poojary, O. Xiang, A. Clearfield, *Chem. Mater.* **2000**, *12*, 294–305; c) B. Gu, L. Wang, S. Wang, D. Zhao, V. H. Rotberg, R. C. Ewing, *J. Mater. Chem.* **2000**, *10*, 2610–2615; d) A. J. Celestian, A. Clearfield, *J. Mater. Chem.* **2007**, *17*, 4839–4842.
- [11] A. L. Spek, *PLATON: A Multi-Purpose Crystallographic Tool*, Utrecht University, Utrecht, The Netherlands, **2001**.
- [12] O. Delgado Friedrichs, M. O’Keeffe, O. M. Yaghi, *Acta Crystallogr. Sect. A* **2003**, *59*, 515–525.
- [13] a) D. Jia, Y. Zhang, Q. Zhao, J. Deng, *Inorg. Chem.* **2006**, *45*, 9812–9817; b) D.-X. Jia, Y. Zhang, J. Dai, Q.-Y. Zhu, X.-M. Gu, *J. Solid State Chem.* **2004**, *177*, 2477–2483; c) V. Spetzler, R. Kiebach, C. Näther, W. Bensch, *Z. Anorg. Allg. Chem.* **2004**, *630*, 2398–2404; d) H.-O. Stephan, M. G. Kanatzidis, *J. Am. Chem. Soc.* **1996**, *118*, 12226–12227; e) K.-S. Choi, M. G. Kanatzidis, *Inorg. Chem.* **2000**, *39*, 5655–5662.
- [14] a) M. J. Manos, R. G. Iyer, E. Quarez, J. H. Liao, M. G. Kanatzidis, *Angew. Chem.* **2005**, *117*, 3618–3621; *Angew. Chem. Int. Ed.* **2005**, *44*, 3552–3555; b) M. J. Manos, K. Chrissafis, M. G. Kanatzidis, *J. Am. Chem. Soc.* **2006**, *128*, 8875–8883.
- [15] N. Zheng, X. Bu, H. Vu, P. Feng, *Angew. Chem.* **2005**, *117*, 5433–5437; *Angew. Chem. Int. Ed.* **2005**, *44*, 5299–5303.
- [16] M. J. Manos, C. D. Malliakas, M. G. Kanatzidis, *Chem. Eur. J.* **2007**, *13*, 51–58.